Wideband equivalent circuits for radial transmission lines

M.B. Steer, B.E., and P.J. Khan, B.Sc., B.E., Ph.D., C.Eng., Sen. Mem. I.E.E.E., F.I.E.R.E., F.I.E. Aust.

Indexing terms: *Transmission line theory, Waves*

Abstract: This paper reports the wideband impedance characteristics of a radial transmission line, in dominant and higher-order modes, and shows how these characteristics can be accurately represented by a lumped-element equivalent circuit.

1 Introduction

The purpose of this paper is to report the wideband impedance characteristics of a radial transmission line, Fig. 1, in dominant and higher-order modes, and to show how these characteristics can be accurately represented by a lumped-element equivalent circuit. The study reported here has direct application to the analysis of harmonic effects in negative-resistance oscillators using packaged diodes, as well as to millimetre-wave circuits using disc-type [1, 2] or bias-pin [3] resonator structures.

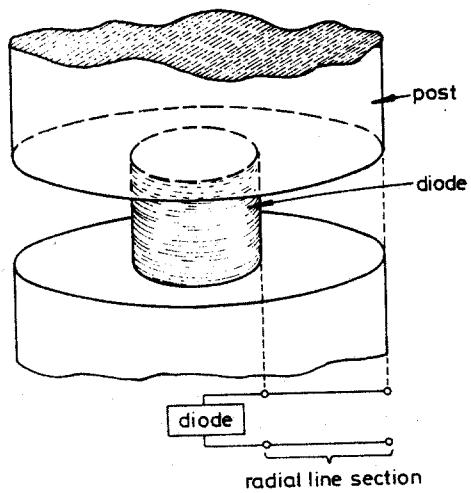

Fig. 1 *Radial transmission line*

Dominant mode radial lines have been discussed previously by Marcuvitz [4], and Ramo, Whinnery and Van Duzer [5].

2 TM mode equivalent circuit deviation

Following the approach of Marcuvitz [4] the E_z and H_ϕ components of a TM_{n1m} outward-travelling radial mode (where the mode is defined as $TM_{\phi rz}$) are readily found to be

$$E_z = A_F H_n^{(2)}(k_c r) \cos\left(\frac{m\pi}{b}\right) z \cos n\phi$$

$$H_\phi = -j\omega\epsilon A_F \frac{1}{k_c} H_n'^{(2)}(k_c r) \cos\left(\frac{m\pi}{b}\right) z \cos n\phi$$

for waves propagating between perfectly conducting plates at $z = 0, z = b$, with

$$k_c = \left[k^2 - \left(\frac{m\pi}{b}\right)^2\right]^{1/2}$$

$H_n^{(2)}(k_c r)$ is the Hankel function of the second kind.

Following the approach of Collin [6] we derive equivalent outward travelling voltage and current waves V^+ and I^+ by

$$E_z = -\epsilon_{om} \frac{V^+}{b} \cos\left(\frac{m\pi}{b}\right) z \cos n\phi$$

$$H_\phi = \epsilon_{on} \frac{I^+}{2\pi r} \cos\left(\frac{m\pi}{b}\right) z \cos n\phi$$

where ϵ_{on} is Neumann's number ($\epsilon_{on} = 1$ for $n = 0$; $\epsilon_{on} = 2$ for $n \neq 0$). This yields

$$V^+ = -\frac{A_F b}{\epsilon_{om}} H_n^{(2)}(k_c r)$$

$$I^+ = -\frac{jA_F\omega\epsilon}{\epsilon_{on}} \frac{2\pi r}{k_c} H_n'^{(2)}(k_c r)$$

By use of the TM radial-mode field relations

$$\frac{\partial E_z}{\partial_r} = \left(j\omega\mu - \frac{1}{j\omega\epsilon}\frac{\partial^2}{\partial_z^2}\right) H_\phi$$

$$\frac{1}{r}\frac{\partial(rH_\phi)}{\partial r} = j\left[\left(\omega\epsilon + \frac{1}{\omega\mu r^2}\frac{\partial^2}{\partial\phi^2}\right) E_z - \frac{1}{r^2\omega\mu}\frac{\partial^2}{\partial\phi\partial z} E_\phi\right]$$

we can express these equations in the standard transmission line form

$$\frac{dV^+}{dr} = -j\beta Z_c I^+; \frac{dI^+}{dr} = -\frac{j\beta}{Z_c} V^+$$

with β as the equivalent phase constant and Z_c the equivalent characteristic impedance of the transmission line.

Carrying out the substitutions we obtain

$$\beta = \left(k_c^2 - \frac{n^2}{r^2}\right)^{1/2}$$

$$Z_c = \frac{\epsilon_{on}}{\epsilon_{om}} \frac{b}{2\pi r} \frac{k_c^2}{\omega\epsilon(k^2 - n^2/r^2)^{1/2}}$$

Since V satisfies Bessel's equation,

$$V(r) = A_n J_n(k_c r) + B_n N_n(k_c r)$$

and

$$I(r) = j\left(\frac{2\pi\omega\epsilon}{bk_c}\right) r \frac{\epsilon_{om}}{\epsilon_{on}} [A_n J_n'(k_c r) + B_n N_n'(k_c r)]$$

Paper 1147H, first received 16th May and in revised form 30th September 1980

The authors are with the Department of Electrical Engineering, University of Queensland, St Lucia, Brisbane, Australia 4067

0143–7097/81/01111 + 03 $01.50/0

obtained from

$$\frac{dV}{dr} = -j\beta Z_c I$$

Using these equations, we can determine the *ABCD* parameters for a length of radial line from $r = r_1$ to $r = r_2$ in the form

$$\begin{bmatrix} V(r_1) \\ I(r_1) \end{bmatrix} = \begin{bmatrix} A(r_1, r_2) & B(r_1, r_2) \\ C(r_1, r_2) & D(r_1, r_2) \end{bmatrix} \begin{bmatrix} V(r_2) \\ I(r_2) \end{bmatrix}$$

with

$$A(r_1, r_2) = \frac{\pi k_c r_2}{2} [N_n'(k_c r_2) J_n(k_c r_1) - J_n'(k_c r_2) N_n(k_c r_1)]$$

$$B(r_1, r_2) = -j \frac{k_c^2 b}{4\omega\epsilon} \frac{\epsilon_{on}}{\epsilon_{om}} [J_n(k_c r_2) N_n(k_c r_1) - N_n(k_c r_2) J_n(k_c r_1)]$$

$$C(r_1, r_2) = j \left(\frac{\pi^2 \omega\epsilon}{b}\right) \frac{\epsilon_{om}}{\epsilon_{on}} r_1 r_2 [N_n'(k_c r_2) J_n'(k_c r_1) - J_n'(k_c r_2) N_n'(k_c r_1)]$$

$$D(r_1, r_2) = \frac{\pi k_c r_1}{2} [J_n(k_c r_2) N_n'(k_c r_1) - N_n(k_c r_2) J_n'(k_c r_1)]$$

The π-equivalent circuit element admittance values are readily found as

$Y_A = (D-1)/B$, $Y_B = (A-1)/B$, and $Y_C = 1/B$, defined in Fig. 2.

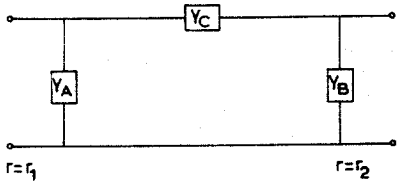

Fig. 2 *General π-equivalent circuit for radial transmission line extending from $r = r_1$, to $r = r_2$*

For the dominant TM mode, these equivalent circuit values reduce to those already given by Marcuvitz [4].

3 TE mode equivalent circuit derivation

The development for the TE mode closely parallels that for the TM mode.

In this case we can derive the equivalent I and V from H_z and E_ϕ, respectively, giving

$$I^+ = \frac{A_F b}{\epsilon_{om}} H_n^{(2)}(k_c r)$$

$$V^+ = \frac{A_F}{\epsilon_{on}} \left(\frac{2\pi r}{k_c}\right) j\omega\mu H_n'^{(2)}(k_c r)$$

The formulas for β and Z_c now become

$$\beta = \left(k_c^2 - \frac{n^2}{r^2}\right)^{1/2}$$

$$Z_c = \frac{2\pi r}{b} \frac{\epsilon_{om}}{\epsilon_{on}} \frac{\omega\mu(k_c^2 - n^2/r^2)^{1/2}}{k_c^2}$$

The current I satisfies Bessel's equation, leading to the expressions

$$I(r) = A_n J_n(k_c r) + B_n N_n(k_c r)$$

$$V(r) = j \left(\frac{2\pi\omega\mu}{bk_c}\right) r \frac{\epsilon_{om}}{\epsilon_{on}} [A_n J_n'(k_c r) + B_n N_n'(k_c r)]$$

from which the *ABCD* parameters are found for a length of line extending from $r = r_1$ to $r = r_2$.

$$A(r_1, r_2) = \frac{-\pi k_c r_1}{2} [J_n'(k_c r_1) N_n(k_c r_2) - N_n'(k_c r_1) J_n(k_c r_2)]$$

$$B(r_1, r_2) = \frac{-j\pi^2 \omega\mu}{b} \frac{r_1 r_2 \epsilon_{om}}{\epsilon_{on}} [J_n'(k_c r_2) N_n'(k_c r_1) - J_n'(k_c r_1) N_n'(k_c r_2)]$$

$$C(r_1, r_2) = \frac{jbk_c^2}{4\omega\mu} \frac{\epsilon_{on}}{\epsilon_{om}} [J_n(k_c r_1) N_n(k_c r_2) - J_n(k_c r_2) N_n(k_c r_1)]$$

$$D(r_1, r_2) = \frac{-\pi k_c r_2}{2} [J_n'(k_c r_2) N_n(k_c r_1) - N_n'(k_c r_2) J_n(k_c r_1)]$$

4 Results

The expressions derived above were applied to investigation of the *X*-band IMPATT oscillator diode mount described by Groves and Lewis [2], which has a resonant-cap structure. The

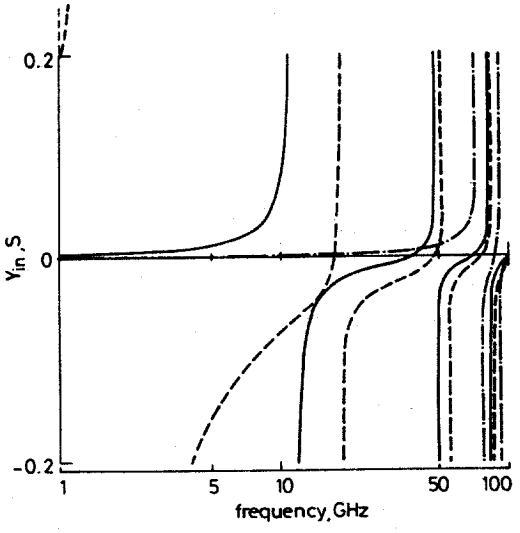

Fig. 3 *Open circuit input admittance of various TM modes*

$r_1 = 0.635$ mm
$r_2 = 5$ mm
$b = 2$ mm

——— TM_{010}
– – – TM_{110}
— · — TM_{111}

radial-line input admittance Y_{in} (evaluated at r_1 with an open-circuit at r_2) was calculated for several TM modes; the oscillation occurs at the frequency for which this susceptance is the negative of that of the diode, neglecting the small contribution from the radiation susceptance at r_2.

Fig. 3 shows the frequency variation of y_{in} for TM_{010}, TM_{110}, and TM_{111} modes. It is evident that the susceptance value differs significantly, between the various modes, above the X-band resonant frequency; this would have an appreciable effect, when an IMPATT diode with a capacitive susceptance is to be tuned by the disc mount. It should be noted that modes such as TM_{110} and TM_{111}, having a circumferential variation in the fields, would be excited if there were a cylindrical assymmetry in the packaged diode, e.g. because of the filamentary lead to the semiconductor. Hence, slight differences in diode package dimensions could lead to spurious responses in a wideband device. The higher-order resonances of y_{in}, for the three modes plotted in Fig. 3, could also give rise to spurious oscillations.

Using the *ABCD* parameters, π-equivalent circuits were obtained for this radial line. The derivation was carried out for only the TM_{010} mode, but the same approach is applicable to other modes. A simple π-equivalent circuit, designed to give an accurate match to the actual radial line admittance at 30 GHz, has the y_{in} values plotted in Fig. 4*b*; comparison with the radial line y_{in}, shown in Fig. 4*a*, indicates that the representation is good only over a very narrow frequency range.

More accurate equivalent circuits were obtained by considering the radial line section to consist of a number of concentric radial segments, or stages, and then obtaining the π-equivalent circuit of each stage. The results for two and four stage equivalent circuits are given in *c* and *d*, respectively, of Fig. 4. These equivalent circuits are reasonably accurare over a larger frequency range than the single-stage circuit. Any degree of accuracy can be obtained by using enough stages.

It has been found empirically that, for a good match of an equivalent circuit to the actual response of a radial line, the radii between the stages must be much less than that derived from the zeroes of the $J_n(k r)$ and $Y_n(k r)$ Bessel functions. Reasonably accurate (typically ± 1%) equivalent circuits can be obtained using the the following procedure, first determine k from five times the highest frequency of interest; second, determine the radii r between the stages from the zeroes of $J_n(k r)$ and $Y_n(k r)$; and third, choose the exact matching frequency to be in the centre of the frequency range. The results for the equivalent circuit obtained using this method, with the highest frequency of interest being 60 GHz, are given in *e* of Fig. 4.

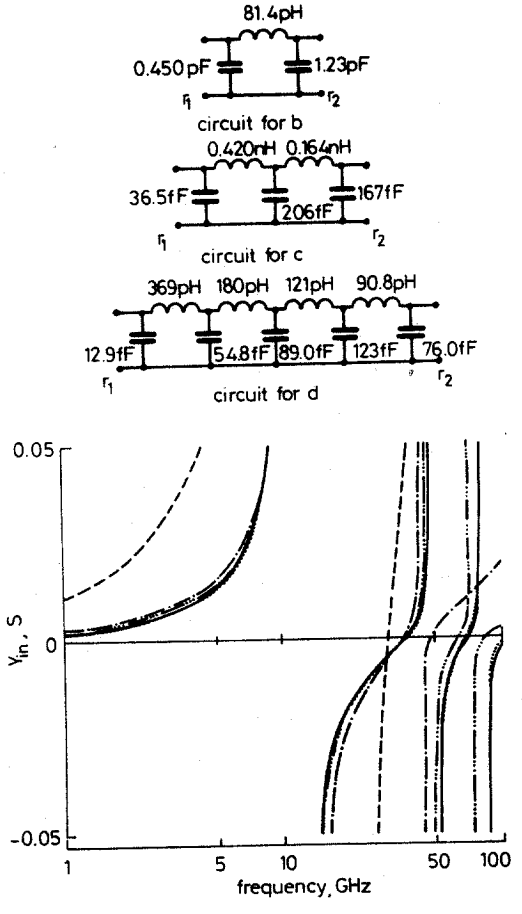

Fig. 4 *Open circuit input admittance of various order equivalent circuits*

$r_1 = 0.635$ mm $r_2 = 5$ mm $b = 2$ mm
a ——— actual dominant TM_{010} mode
b – – – – 1-stage equivalent circuit
c — · — 2-stage equal section equivalent circuit
d — · · — 4-stage equal section equivalent circuit
e · · · · 19-stage equivalent circuit obtained using the empirical method for an accurate equivalent circuit with 60 GHz the highest frequency of interest. Matching frequency = 30 GHz.

5 Conclusion

This paper presented the derivation of lumped-element equivalent circuits for radial transmission lines, valid over a wide frequency range. Any desired accuracy or bandwidth of these equivalent circuits can be obtained. A procedure was presented for the quick determination of accurate equivalent circuits. These circuits can be used to obtain better equivalent circuits of diode mounts than have hitherto been available.

It was seen that resonances of unwanted radial modes may fall in the desired operating frequency range of devices. This has implications for the performance of oscillators and wide-band devices.

6 Acknowledgments

This work was supported by United States ARO Grant DAA G29-76-G-0279 and Australian Research Grants Committee Grant F 76/15147.

7 References

1 LEE, T.P., STANLEY, R.D. and MISAWA, T.: 'A 50 GHz silicon IMPATT diode oscillator and amplifier', *IEEE Trans.*, 1968, ED-15, pp 741–747
2 GROVES, I.S., and LEWIS, D.E.: 'Resonant-cap structures for IMPATT-diodes', *Electron. Lett.*, 1972, pp 98–99
3 WELLER, K.P., YING, R.S., and LEE, D.H.: 'Millimetre IMPATT sources for the 130–170 GHz range', *IEEE Trans.*, 1976, MTT-24, pp 738–743
4 MARCUVITZ, N.: 'Radial transmission lines', *in* MONTGOMERY, C.G., DICKE, R.H., and PURCELL, E.M. (Eds.): Principles of microwave circuits, MIT radiation Lab. Series (McGraw-Hill, 1947) Chap. 8, pp. 240–282
5 RAMO, S., WHINNERY, J.R., and VAN DUZER, T.: 'Fields and waves in communication electronics' (John Wiley and Sons, 1965), pp. 453–460
6 COLLIN, R.E.: 'Foundations for microwave engineering' (McGraw-Hill, 1966), pp. 145–148